Multichromophores Onto Graphene: Supramolecular Non-Covalent Approaches for Efficient Light Harvesting.

Solon P. Economopoulos* and Nikos Tagmatarchis*

Theoretical and Physical Chemistry Institute, National Hellenic Research Foundation, 48 Vassileos Constantinou Avenue, 11635 Athens, Greece.

Fax: + 30 210 7273794; Tel: + 30 210 7273835

ABSTRACT. The idea of attaching multiple porphyrins to graphene is explored. A charged porphyrin salt is stabilized onto exfoliated graphene by taking advantage of π-π* interactions and a second porphyrin light harvester is anchored through electrostatic interactions with the former. The interactions are capable of allowing electronic communication of the second, electrostatically attached, porphyrin with graphene, effectively quenching its emission. The graphene-porphyrin-porphyrin triad is examined through optical (UV-Vis, steady state and time resolved photoluminescence) techniques, while electrochemistry is employed to study the thermodynamically favored pathways through which the interaction occurs. The porphyrin that is electrostatically stabilized onto the graphene nanoensemble shows lifetimes one order of magnitude faster than its π-π* stacked analogue suggesting a more efficient pathway.

1.INTRODUCTION

The isolation of a single sp^2 single layer of graphene from graphite by Manchester's research team, has received tremendous scientific acceptance from the community since its introduction in 2004,[1] culminated by the Nobel prize in physics awarded in 2010. Owing to its superior mechanical and electronic properties, graphene and its most widely used derivative, graphene oxide[2] is quickly filling a niche spot[3] for nanomaterials in a variety of optoelectronic[4], biological[5] mechanical reinforcing,[6] as well as, other[7] interesting applications. Despite the intense research interest revolving around graphene applications, several obstacles have to be overcome, as with any new material, before any real discussion on commercial applications can commence. The premium hurdle at this stage revolves around the facile mass production of graphene. This problem seems to be tackled on rather effectively either through the intermediate stage of graphene oxide (albeit with a considerable degradation of many desirable properties of the material due to the number defects introduced) or as a direct product of graphite (or expanded graphite) exfoliation, exemplified lately by a variety of excellent projects.[8] However, the continuous effort towards the end-goal of mass production is continually fueled by the various applications of graphene which, at the moment, require different approaches with respect to graphene synthesis.[9] Another obstacle towards widespread incorporation of graphene stems from its poor processability allowing for difficulty in forming high quality single layers sheets in areas anything other than a few mm^2. Korean research groups have worked extensively on this issue achieving key milestones,[10] while, recently, an interesting approach at producing, fairly large, free standing CVD-grown graphene films has been proposed.[11] When looking into the uses of graphene from the point of view of a material scientist, liquid exfoliation of graphite, to produce graphene,[12] offers several distinct advantages. It provides a facile way of generating gram-scale quantities of the material and it delivers a solution-based product, which is extremely useful once

we consider subsequent chemical functionalization. More importantly, the quality of the produced material, both in particle size and number of layers, poses no significant drawbacks that would limit its uses, in this particular scientific area. At the same time the produced graphene flakes possess fewer defects and thus retain most of their electronic properties, compared to graphene oxide.

In the subject of covalent and non-covalent graphene functionalization with chromophores, the possibilities are virtually limitless with extensive research, actively, being pursued.[13] When supramolecular interactions, with the objective to minimize the damage to the graphitic plane, are taken advantage of, in order to integrate organic moieties to graphene, the resulted hybrids suffer from the weaker π-π* interactions and the presence of unattached free-standing organic units in the solution. However the extended aromatic lattice of graphene sheets remains intact and undisrupted, as no bond formation takes place, as is the case in the covalent attachment of organic units, thus allowing for the preservation of graphene's electronic properties (e.g. ballistic transport of charges with negligible loss of energy etc). Considering non-covalent functionalization of graphene, several reports have been published incorporating a wide family of chromophores. Due to its similarities with the graphene structure and its excellent π-π* stacking properties, the pyrene unit seems to be a favorite among non-covalent interaction studies with graphene reported in multichromophores with p-phenylenevinylene (PPV) derivatives,[14] azobenzene chromophores,[15] phthalocyanines and porphyrins[16] as well as Co(II) bis-terpyridyl complexes.[17] Other chromophores include PPV oligomers with pendant phthalocyanine rings[18] and dendrimers bearing perylene bisimide[13b] that have been incorporated for the preparation of supramolecular graphene-based nanoensembles promoting stabilization. Taking into account the rapid formation of the non-covalently attached nanoensembles of

graphene, this route is particularly useful in rapid screening for evidence of electronic communication between the selected chromophore and the carbon nanostructure.

Porphyrins, on the other hand, have a long track record in academic research with multiple Nobel-awards revolving around their biological properties, while their use in photovoltaics, in particular, continues to set impressive benchmarks.[19]

The field of research revolving around anchoring multiple chromophores is extremely attractive, but also relatively challenging. The idea is to design a system of antennas in order to provide a simple, yet elegant, approach for enhanced spectral coverage across the visible (and near-infrared) spectrum regions that can maximize contribution to solar light harvesting *via* an energy or charge transfer cascade to the electron acceptor. Several interesting works have emerged, dealing with the efficient solar absorption when incorporating more than one chromophore in a system. The groups of D'Souza and Ito have reported on the integration of multichromophores in fullerenes and carbon nanotubes[20] through covalent and non-covalent techniques and their potential, while several synthetic attempts for covalent attachment in fullerenes[21] and carbon nanostructures[22] have also been presented.

While the literature surrounding porphyrins and graphene is fairly active,[23] in this paper we explore the incorporation of multiple chromophores onto exfoliated graphene layers. To the best of our knowledge this is the first report on dual porphyrin-functionalized graphene with only the research team of Guldi dealing with non-covalent attachment of multichromophores onto graphene.[24] The chromophores are anchored via non-covalent interactions, taking advantage of the well established π-π^* interactions between carbon nanostructures and porphyrinoids i.e. porphyrins[25] and phthalocyanines.[26] This report provides a definitive proof of concept that

instead of synthesizing a single chromophore attached onto graphene a careful selection and anchoring of multiple chromophores, spanning the visible spectrum, is possible.

2. EXPERIMENTAL SECTION

Graphite flakes were supplied from Aldrich and were used without additional treatment before sonication. N-methyl pyrrolidone (NMP) was supplied from Aldrich, H_2O (HPLC grade) was supplied from Fluka. Sonication was performed on a Bandelin Sonoplus Ultrasonic Homogenizer HD 3200 equipped with a flat head probe (VS70T), running at 10% of the maximum power (250 W). UV-Vis-IR electronic absorption spectra were recorded on a Perkin–Elmer (Lambda 19) UV-Vis-NIR spectrophotometer. Raman scattering measurements were performed in the backscattering geometry using a RENISHAW inVia Raman microscope equipped with a CCD camera and a Leica microscope at room temperature. A 2400 lines per mm grating was used for all measurements, providing a spectral resolution of $\pm 1 cm^{-1}$. As an excitation source the Ar^+ laser (514 nm with less than 0.5 mW laser power) was used. Measurements were taken with 120 s of exposure times at varying numbers of accumulations. The laser spot was focused on the sample surface using a long working distance 50x objective. Raman spectra were collected on numerous spots on the sample and recorded with a Peltier cooled CCD camera. The intensity ratio I_D/I_G was obtained by taking the peak intensities following any baseline corrections. Electrochemistry studies were performed using a standard three-electrode cell with Pt disk (1.6 mm diameter) as a working electrode, Pt mesh as counter-electrode and Pt wire as a pseudo reference electrode. Cyclic voltammograms were carried out in dried NMP using $TBAPF_6$ (recrystallized three times from acetone and dried in vacuum at 100 °C before each experiment) as electrolyte, under N_2 atmosphere. Ferrocene was used as an internal standard for all measurements. Voltammograms were recorded using an EG&G Princeton Applied Research potensiostat/galvanostat model 2273

connected to a personal computer running PowerSuite software. The energy levels of the materials were calculated using the following equations.[27]

$E_{HOMO} = (E_{[onset,ox\ vs.\ Fc/\ Fc^{+}]} + 5.1)$ (eV)

$E_{LUMO} = (E_{[onset,red\ vs.\ Fc/\ Fc^{+}]} + 5.1)$ (eV)

For ease of reference all values are reported as absolute values.

Steady-state emission spectra were recorded on a Fluorolog-3 Jobin Yvon-Spex spectrofluorometer (model GL3-21). Picosecond time-resolved fluorescence spectra were measured by the time-correlated single-photon counting (TCSPC) method on a NanoLog spectrofluorometer (Horiba Jobin Yvon), using a laser diode as an excitation source. (NanoLED, 376 nm, 200 ps pulse width) Lifetimes were evaluated with the DAS6 Fluorescence-Decay Analysis Software. The minimum value for the fluorescence rate constant k_f and fluorescence quantum yield Φ_f were also calculated, based on the following equations.

(Eq. 1) $k_f = (1/\tau_f)_{nanoensemble} - (1/\tau_f)$chromophore, where τ_f is the fluorescence lifetime

(Eq. 2) $\Phi_f = k_f/(1/\tau_f)_{nanoensemble}$, where τ_f is the fluorescence lifetime

General synthetic process for the graphene porphyrin nanoensembles A and B. Graphene was exfoliated through the use of a tip sonicator by adding 20 mg of graphite flakes in 10 mL of NMP. The formation of the water soluble poprhyrin-graphene nanoensembles was accomplished by obtaining graphene through liquid-phase exfoliation, using NMP, filtering to remove the solvent and re-dispersing the solid product in a 10^{-3}M solution of the aqueous solution of the porphyrin. The mixture was mildly sonicated and left to stir for 24h and then centrifuged for 30

min at 4000 rpm. The supernatant contained no visible amount of graphene and it was discarded to remove the excess of porphyrin. The precipitate was re-dissolved in H_2O, sonicated for 15 min, yielding a dark suspension the formed nanoensemble, which was stable for several days. Due to the nature of the experiments for different repetitions of the experiments, newly prepared graphene-porphyrin nanoensembles were prepared each time, in order to avoid precipitation.

General process for the formation and optical characterization of the graphene-porphyrin-porphyrin triad. In a quartz cuvette, a suitable concentration of the porphyrin (10^{-5} M for the anionic porphyrin **I** or 10^{-6} M for the cationic porphyrin **II)** were added. The solution was measured in respect to their absorption and emission properties and the respective graphene-porphyrin nanoensemble **B** or **A**, was added gradually, each time measuring the changes in the optical properties and the photoluminescence lifetimes.

3. RESULTS AND DISCUSSION

The structures of the porphyrins used in the current study are depicted in Scheme 1. Briefly, the porphyrin **I** is a sodium salt consisting of a porphyrin ring decorated with 2 carboxy anion groups, while the cationic porphyrin **II** consists of a porphyrin ring with four methyl pyridine groups peripherally, stabilized with four p-methyl phenyl sulfonate anions. The core methodology followed revolved around the synthesis of a stable water soluble graphene-porphyrin nanoensemble (Scheme 1) and the study of a possible electrostatic interaction with graphene of an oppositely charged porphyrin, once it was introduced, to the formed nanoensemble. The resulting porphyrin-porphyrin-graphene triad was investigated using optical techniques such as UV-Vis, PL and time-resolved fluorescence.

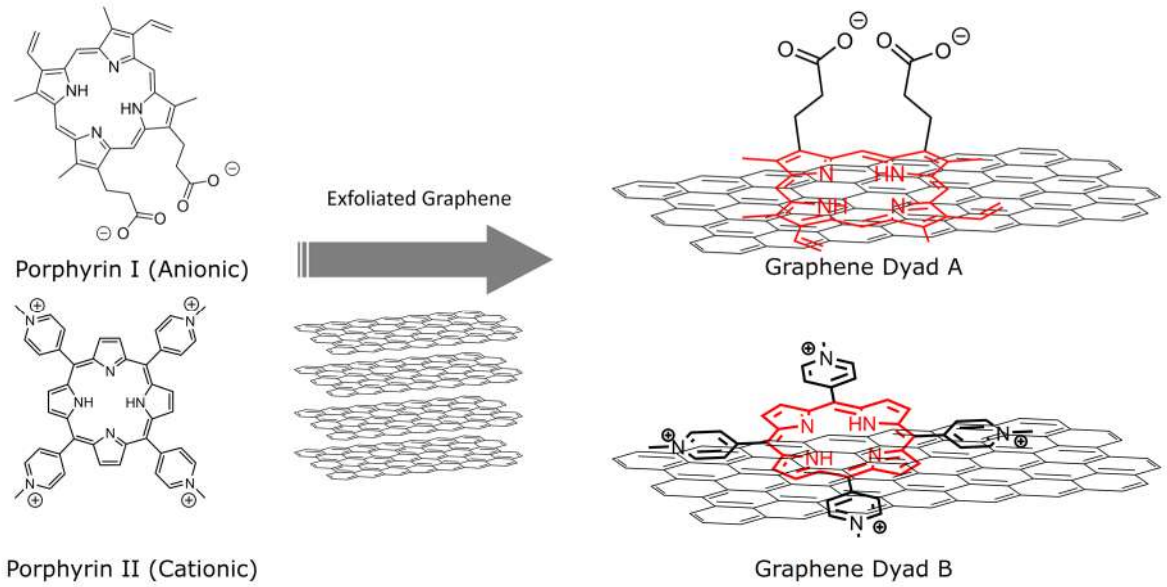

Scheme 1. Schematic representation of porphyrins **I** and **II** examined and the proposed graphene-porphyrin nanoensembles **A** and **B** formed.

The synthesis of the graphene-porphyrin dyads **A** and **B** is taking advantage of the well-established interactions of 2D conjugated systems with graphene.[13c, 24, 28] The synthesis of the water soluble nanoensembles holds two key-steps. The first is the removal of the organic solvent (in this case NMP, but benzylamine[29] can also be used with no differentiation in the end product) and the transfer of the exfoliated graphene to water. The second is the removal of the excess porphyrin that did not interact with graphene through π-π* stacking. The former obstacle can be addressed through the filtration of the exfoliated graphene in NMP. A thorough washing of the black solid with water should ensure that most of the organic solvent is removed. Due to the nature of the exfoliating process it is inevitable that some of the solvent will remain trapped between few-layer graphene sheets, or attached to graphene. This however does not interact with the solubilization of graphene in water. In a simple blank experiment, exfoliated graphene in

NMP was filtrated, not washed (in order to ensure that as much of the organic solvent remains attached to graphene) and the black powder was sonicated in water. After centrifugation, (5 min at 4400 rpm) a practically clear solution was obtained with the graphene precipitating. This reveals that any residual solvent does not interact with the solubility of exfoliated graphene in water, but such a phenomenon occurs solely as a result of the interaction of graphene with the water soluble porphyrin salts **I** and **II** and the formation of non-covalent interactions. On the latter step of the formation of graphene porphyrin nanoensembles **A** and **B**, the removal of the excess of unreacted porphyrin with graphene is achieved with an intermediate centrifugation step (see Experimental section) of the product, in which the main objective is to remove the bulk of the solvent and, therefore, the unreacted porphyrin without losing too much of graphene-porphyrin nanoensemble. The nanoensembles **A** and **B** were characterized and their differential pulse voltammograms are depicted in **Figure S1** while their time-resolved spectra are shown in **Figure S2**. The data are summarized in **Table I**.

Table I. Redox data, fluorescence lifetimes and the fluorescence rate constant and fluorescence quantum yield for the porphyrin salts and the graphene nanoensembles **A** and **B.**

Material	E_{red}	LUMO	τ_f (ns)	τ_f (ns)	k_f (s^{-1})	Φ_f
Anionic Porphyrin **I**	-1.75 V	3.5 eV	15.2 ns			
Cationic Porphyrin **II**	-1.82 V, -1.00 V	4.2 eV	5.1 ns			
Graphene nanoensemble **A**	-1.75 V, 0.50 V		15.2 ns	2.8 ns	$2.9\ 10^8$	78.4
Graphene nanoensemble **B**	-1.81 V, -1.00 V, 0.50 V		5.2 ns	1.6 ns	$4.3\ 10^8$	68.8

The graphene nanoensembles **A** and **B** were also characterized using HR-TEM microscopy to determine whether the exfoliation and the porphyrin-graphene π-π* stacking process was

efficient in the production of few-layered and single-layer graphene sheets. The microscopy images from the nanoensembles **A** and **B** are presented in **Figure 1**. In **Fig 1a** the HR-TEM image of grapheme nanoensemble is shown with a zoom in on the edge of the sheet. Imaging obtained through Selected Area Electron Diffraction and the Fast Fourier Transform (SAED-FFT) of the selected area, (inset) confirms that this is single-layer graphene. The graphene nanoensemble B's image is shown in **Fig 1b** showing the edge of the single layer of graphene, as SAED-FFT (inset) verifies. These are not typical HR-TEM images and, naturally, not all of the graphene nanoensembles produced are comprised of single-layered graphene. There are few-layer graphene sheets, graphene sheets loaded with organic content etc. More TEM images from materials **A** and **B** showing the single and few-layered graphenes obtained, are presented as supporting information. (Figures **S3** and **S4**) However the obtained images solidify our assumption that we can produce high-quality exfoliated graphene in NMP and successfully switch the solubility, with the aid of the porphyrin salts, forming stable high quality aqueous nanoensembles.

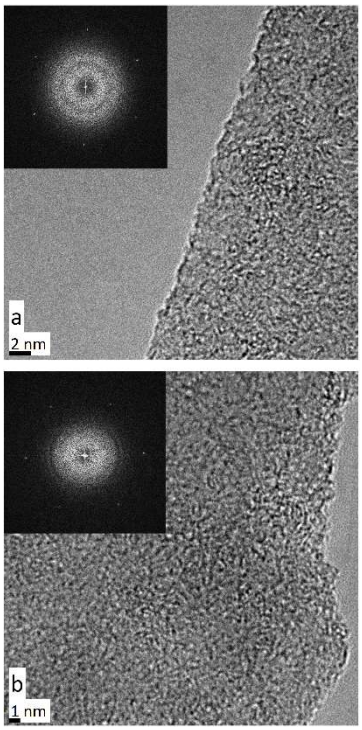

Figure 1. HR-TEM images of a) nanoensemble **A**, and b) nanoensemble **B**. Insets: SAED-FFT pattern showing single-layered graphene sheets.

Due to the nature of this series of experiments, it is worth exploring the possible thermodynamically favorable routes that this double-porphyrin graphene system possesses. To this end, electrochemistry was employed to determine the energy levels of the two porphyrins and nanoensembles, along with graphene to determine what charge/energy transfer mechanisms can be favoured. From the differential pulse voltammetry (DPV) data (**Figure S1a**) we can clearly detect a reduction at -1.75 V, attributed to the porphyrin moiety, which yields a LUMO level of around 3.5 eV. A broad reduction peak centered at around -0.5 eV can be attributed to the carbon nanostructure. For the nanoensemble **B**, (**Figure S1b**) the DPV shows two distinct reduction peaks at -1.82 V, and -1.0 V and a broad reduction at around 0.5 V. The reduction at -1.82 V can be attributed to the porphyrin ring, while the sharp peak at -1.0 V can be assigned to

the four methyl pyridine groups present. The reduction at -1.0 V yields a LUMO of around 4.2 eV. The broad reduction at around -0.5 V can be attributed the graphene particles. From the electrochemical data collected we can conclude the following thermodynamically favored scheme. The cationic porphyrin **II** can allow charge/energy transfer from porphyrin **I**, while the opposite is thermodynamically forbidden.

Both porphyrins' emission can be quenched by graphene. In order to explore the possibility of electrostatic interaction between the oppositely charged porphyrins, a dilute solution 10^{-5} or 10^{-6} M of the porphyrins **I** and **II**, respectively, was used. To this solution, the respective nanoensemble constisting of the oppositely charged porphyrin and graphene was added and the effect to the PL intensity and the lifetime of the excited species of the poprhyrin was investigated. From the data of the pristine porphyrin **I** there are two characteristic emission peaks. The larger emission peak is located at 621 nm, while a smaller intensity peak is seen at 683 nm. The cationic porphyrin **II** exhibits a single emission peak with a maximum at 712 nm. Also worth noting is the fact that the latter porphyrin **II** has a higher quantum efficiency than porphyrin **I**, by a factor of at least ~100. This is the reason that we opted to use a more dilute 10^{-6} M solution for porphyrin **II**, compared to porphyrin **I** (10^{-5} M).

In **Figure 2**, the emission spectra of the porphyrins **I** and **II** are presented, upon addition of the graphene nanoensembles **B** and **A**, respectively

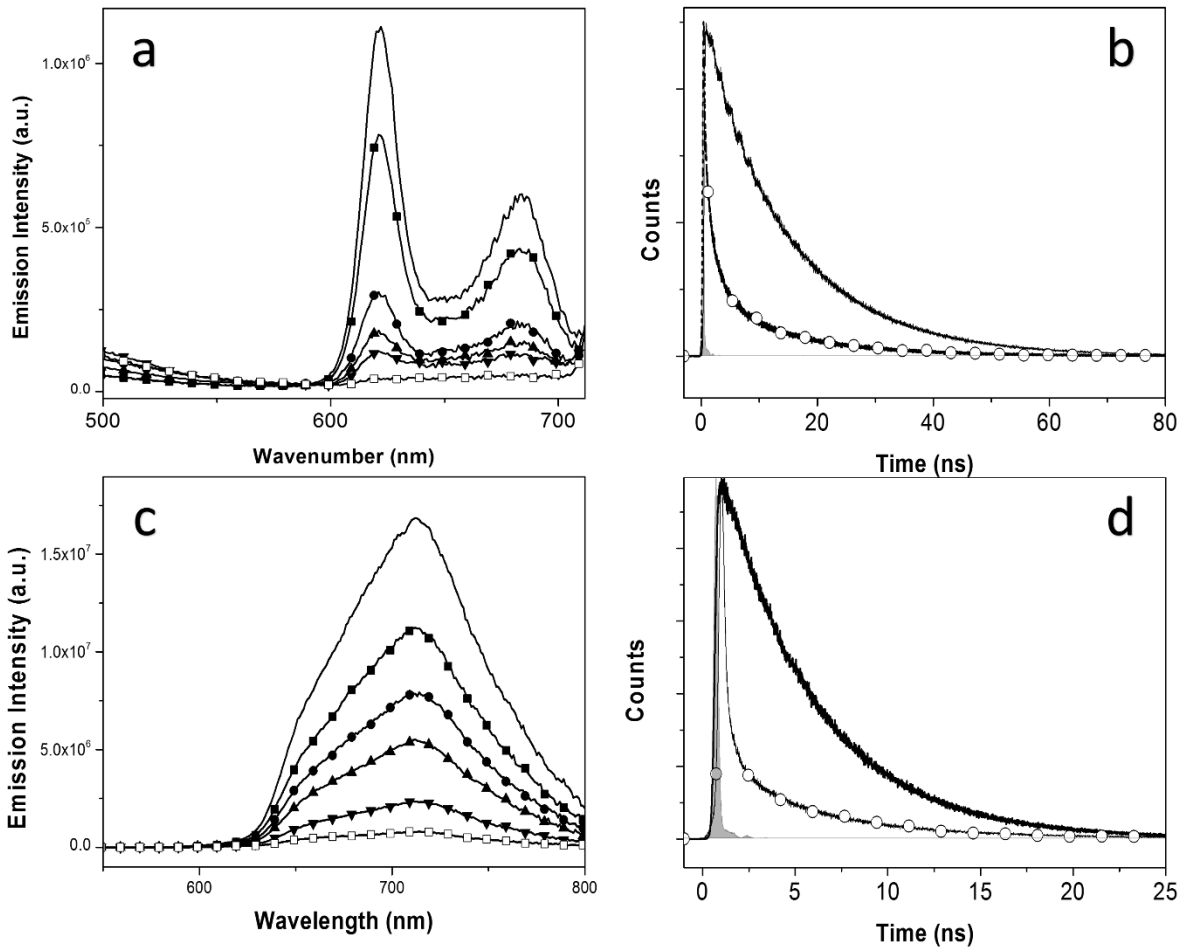

Figure 2. a) Emission of anionic porphyrin **I** (solid line) with increasing addition of graphene nanoensemble **B** (2, 4, 6, 8 and 10 μL, respectively), and b) decay fluorescence lifetimes of anionic porphyrin **I** 10^{-5} M (black line) and upon 10 μL addition of graphene nanoensemble **B**. (-○-) c) Emission of cationic poprhyrin **II** (solid line) with increasing addition (10, 20, 30, 50 and 70 μL, respectively) of graphene nanoensemble **A**, and d) decay fluorescence lifetimes of cationic porphyrin **II** 10^{-6} M (black line) upon 70 μL addition (-○-) of graphene nanoensemble **A**. All spectra obtained in H_2O solutions. Steady state spectra were obtained by excitation in the maximum of their respective UV absorption peaks (375 and 421 nm respectively). Time resolved data obtained using 376 nm excitation line.

From the data presented in **Figure 2** (a and c) it is clear that the graphene nanoensembles quench the porphyrin solutions very efficiently by a factor of ~50 in each case. Very small quantities, in the order of μL, are sufficient to minimize the emission intensity, while not affecting, significantly, the final concentration of the solution (to the point that the observed decrease in emission intensity can be attributed to this factor). This is a first indication that even in dilute solutions such as these, electrostatic interactions between the oppositely charged porphyrins can take place. On another note it is clear that different amounts of graphene nanoensembles are needed to quench the porphyrin. This trend was evident in every series of experiments with different batches of graphene ensembles where, naturally, the concentration of the nanoensemble could not be precisely duplicated from one batch to the next. In every case the amount in μL of the nanoensemble used to quench the porphyrin **II** was in the order of x5-x7 compared to the amount needed to quench anionic porphyrin **I**. However this differentiation on the behavior did not affect the reproducibility of the observed trend in each case. Further insight from these experiments derives from time resolved photoluminescence experiments conducted in these solutions. The data collected are shown in **Figure 2** (b and d) while the lifetime values are summarized in **Table II**.

Table II. Decay fluorescence lifetimes, fluorescence rate constant and fluorescence quantum yields calculated from **Figure 2a** for the anionic porphyrin I upon gradual addition of graphene nanoensemble B and decay fluorescence lifetimes for the cationic porphyrin II upon gradual addition of graphene nanoensemble A (**Figure 2b**).

Material	τ_f (ns)	τ_f (ns)	τ_f (ns)	$k_{f\,(}s^{-1})$	Φ_f
Pristine Anionic Porphyrin	15.1 ns				
+10μL of nanoensemble B	14.7 ns	2.4 ns	0.2 ns	$4.5\ 10^9$	0.9
Pristine Cationic Porphyrin	5.1 ns				

+70 μL of nanoensemble A	5.7 ns	0.3 ns	-	3.1 10^9	0.93

Focusing on **Fig. 2b** and expanding on the observations derived from our results, we can clearly deduce, by analyzing the single exponential curve of the pristine anionic porphyrin, that the lifetime of the chromophore is around ~15 ns. Once the graphene nanoensemble **B** is introduced in the aqueous solution, there is a significant shift in shape in the exponential curve obtained. Three distinct components can exist in the solution and are responsible for emitting light at 621 nm. The pristine free-standing anionic porphyrin **I**, the anionic porphyrin **I** directly interacting with graphene *via* non-covalent attachment and the proposed triad of the anionic porphyrin **I** interacting with graphene *via* the electrostatic bridging of the cationic porphyrin **II**. By using a tri-exponential decay curve analysis, we obtain the best chi-squared value and we can calculate the lifetimes of these components. The first lifetime is calculated at around 15 ns, and is attributed to the free-standing porphyrin, the second lifetime is in the order of 3 ns and is attributed to the interaction of the anionic porphyrin with graphene (**Table I**) and the final component seems to have a much shorter sub-1 ns lifetime and can be evidence of the interaction of the anionic porphyrin **I** through the electrostatic bridging with graphene *via* the cationic porphyrin **II** and the formation of the proposed triad. On the next series of experiments involving cationic porphyrin **II** and graphene nanoensemble **B**, the data are summarized in **Table II**. Looking at the analyzed data obtained from Figure **2d** we observe, firstly, the mono-exponential decay of the pristine cationic porphyrin, as expected, yielding a calculated lifetime of ~5 ns. The observation that stands out is that once the addition of the graphene nanoensemble **A**, quenches the emission of the porphyrin, a tri-exponential decay analysis fails to accurately calculate the lifetimes, yielding either too high chi-squared values or lifetime values that cannot be assigned to

any component in the system. The only analysis that allows chi-squared values close to 1 (from 1.00 to 1.49) is a bi-exponential analysis. This shows that two components basically exist in the system. One component has a lifetime of around 5 ns assigned to the pristine cationic porphyrin **II** while the other very fast component has a lifetime of 0.3-0.4 ns that can be assigned to the formation of the triad. In this case the fastest component can be assigned to the interaction of the porphyrin **II** with graphene *via* the electrostatic interactions with porhyrin **I**, thus providing additional evidence on the formation of the triad. Also worth mentioning is that upon lower volumes of graphene nanoensemble **A** added, the bi exponential decay analysis, shows the lifetime of the pristine free standing porphyrin **II** at ~5.5 ns and a lifetime of around 1.5 ns, attributed to the formation of π-π stacked porphyrin **II** onto graphene.

In order to elucidate and solidify our results additional experiments needed to be carried out. First and foremost we have observed that the formation of the triad is happening very fast. As soon as each of the nanoensembles is added, the results are evident, both in steady state and time-resolved luminescence experiments. This raises the question of whether the addition of a small amount, in the order of μL, of exfoliated graphene in NMP, to a solution of porphyrins **I** and **II** should yield the same results. The central idea behind this series of experiments is to form *in situ* the graphene-porphyrin-porphyrin triad, in solution. To this end, we prepared an aqueous 10^{-6} M solution of the cationic porphyrin and added twice the amount of the anionic porpyrin. The 10^{-6} M concentration was chosen, taking into account that the emission of the cationic porphyrin will be predominantly visible due to the increased quantum efficiency of the molecule. The 2:1 ratio chosen for the anionic and cationic porphyrins **I** and **II**, respectively, aims at neutralizing the negative and positive charges of the two chromophores, as porphyrin **I** has a total charge of -2, while porphyrin **II** has a total charge of +4. The notion is to create *in situ* a

dyad of the two porphyrins and to examine the possibility of exfoliated graphene to interact with the dyad (Scheme 2).

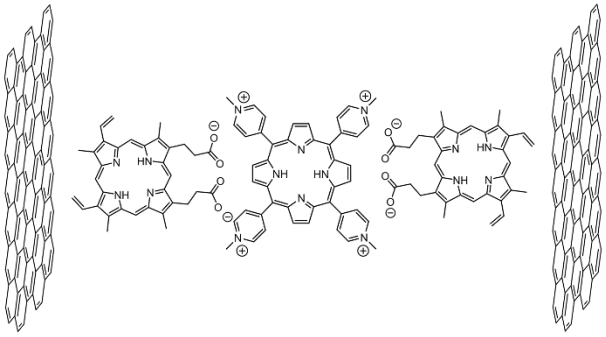

Scheme 2. Schematic representation of the proposed anionic porphyrin **I** and cationic porphyrin **II** dyad formed and the subsequent π-π* interactions with exfoliated graphene.

To this end, a mixture of the two porphyrins, was prepared in a 2:1 ratio (anionic:cationic respectively) and exfoliated graphene in NMP was added and the emission of porphyrin **II** was monitored. The steady-state emission data are presented in **Figure 3**.

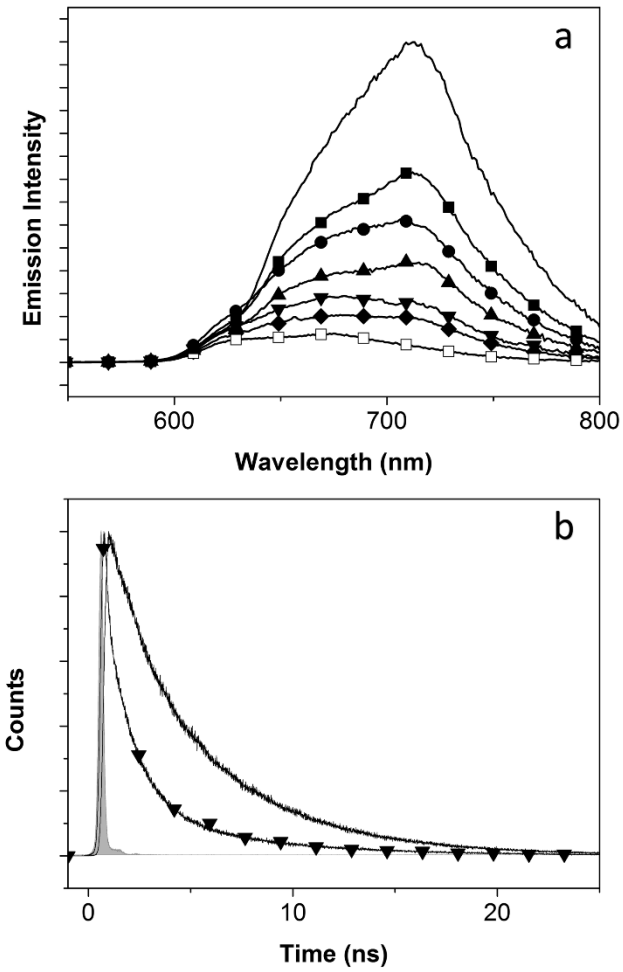

Figure 3. Porphyrin **I** and porphyrin **II** 10^{-6} M pristine solution (solid line) upon gradual addition of exfoliated graphene in NMP. a) Steady-state photoluminescence spectra with 2, 4, 6, 8, 10 and 20 μL of exfoliated graphene added, respectively (excitation 421 nm), and b) decay fluorescence lifetimes of the two chromophores (black line) and upon addition of 10μL of exfoliated graphene (-▼-).

From **Fig. 3a** it is clearly evident that in the starting 2:1 solution the emission of the porphyrin **II** dominates this part of the spectra. The anionic porphyrin's (**I**) emission at 621 nm is overlapped. As a sidenote it is worth noting that the absolute emission intensity of the porphyrin remains virtually unchanged whether it is examined in pristine form, or in a mixture with anionic porphyrin

I. This indicates that no charge or energy transfer takes place due to porphyrin stacking and poprhyrin aggregates forming, that can cause emission quenching. Thus any such phenomena can be solely attributed to the presence of the carbon nanostructure. Upon addition of exfoliated graphene, the emission of the porphyrin is reduced by almost 50% and further addition of graphene causes a twenty-fold reduction of photoluminescence. The excitation line used for the photoluminescence measurements is 421 nm, centered on the Soret band the cationic porphyrin **II** and avoiding excitation of the anionic porphyrin **I**, whose absorption maxima lies around 380 nm. The data from the time-resolved spectra in **Figure 3b** are summarized in **Table III**.

Table III. Decay fluorescence lifetimes, fluorescence rate constant and fluorescence quantum yield for the anionic porphyrin I: cationic porphyrin II mixture upon gradual addition of exfoliated graphene (**Figure 3b**).

Materials	τ_f (ns)			$k_{f\,(s^{-1})}$	Φ_f
Anionic : Cationic Porphyrin 2:1	5.4 ns				
+ 10 μL of Graphene	6.3 ns	1.4 ns	0.2 ns	$4.8\ 10^9$	0.96

From the analysis of the time-resolved spectra we can clearly discern 3 components. The first component has a lifetime of ~5 ns and is attributed, as expected, to the cationic porphyrin. A much faster component in the order of 1-2 ns can be assigned to the graphene cationic nanoensemble **B**. In small quantities of graphene added a lifetime of 2.4 ns calculated, suggests that the component might be attributed to the formation of graphene nanoensemble **A**, however, the emission of 712 nm that we probe the sample suggests that the anionic porphyrin emission cannot be used to explain this lifetime and that this is simply a matter of the calculation algorithm of the software. Finally, as is the case with the previous samples, there is a very fast component that can be attributed to the formation of the triad. As we increase the graphene

concentration the population of this components is altered. Fewer molecules of the free porphyrin remain while the majority of the emission stems from the formation of the graphene nanoensemble **B**. The population of the triad also increases. Notably, if we compare the results to the ones obtained in the series of experiments presented in **Figure 2b** and **Table II** it is clear that much less volume of graphene is consumed to quench the emission and form the components, although the concentrations of graphene cannot be accurately measured.

CONCLUSIONS

We demonstrate electronic communication of exfoliated graphene with chromophores electrostatically anchored onto the graphitic backbone. The chromophores are attached with another chromophore which is non-covalently anchored onto graphene demonstrating one of the very few multichromophore water soluble graphene-based donor-acceptor nanoensembles. The system exhibits efficient quenching of the electrostatically attached porphyrins hinting at either charge or energy transfer phenomena taking place between the two components. The analysis of the formed dyads and triads is currently examined using fs transient absorption spectroscopy in order to further elucidate the nature and the mechanism of the observed phenomena and the results will be reported shortly. The non-covalent functionalization of graphene leaves its electronic properties unaffected, while the water solubility and the formation of stable suspensions of the triads opens up a variety of interesting optoelectronic applications. Moreover the faster component indicated in every case of the nanoensembles examined indicates that the interaction between the electrostatically anchored porphyrin and the carbon nanostructure is more efficient than its π-π^* stacked analogue.

Supporting Information. Electrochemical data for the graphene nanoensembles, decay fluorescence lifetimes for the dyads **A** and **B,** additional HR-TEM images of the dyads and optical absorption spectra are included in the supporting information section. This material is available free of charge via the Internet at http://pubs.acs.org.

Corresponding Authors

*Emails: economop@eie.gr (S. P. Economopoulos); tagmatar@eie.gr (N. Tagmatarchis)

ACKNOWLEDGMENT

The authors gratefully acknowledge financial support from GSRT/NSRF 2007-2013 through action "Supporting Postdoctoral Researchers" project GRAPHCELL PE5(2126) by the Greek General Secretariat for Science and Technology. We are also indebted to the group of Prof. H. Shinohara, Nagoya University, Japan, for access to their TEM facilities and performing the imaging of the materials.

1. Novoselov, K. S.; Geim, A. K.; Morozov, S. V.; Jiang, D.; Zhang, Y.; Dubonos, S. V.; Grigorieva, I. V.; Firsov, A. A., Electric Field Effect in Atomically Thin Carbon Films. *Science* **2004,** *306* (5696), 666-669.

2. Dimiev, A. M.; Tour, J. M., Mechanism of Graphene Oxide Formation. *ACS Nano* **2014,** *8* (3), 3060-3068.

3. Novoselov, K. S.; Falko, V. I.; Colombo, L.; Gellert, P. R.; Schwab, M. G.; Kim, K., A roadmap for graphene. *Nature* **2012,** *490* (7419), 192-200.

4. (a) Liu, M.; Yin, X.; Ulin-Avila, E.; Geng, B.; Zentgraf, T.; Ju, L.; Wang, F.; Zhang, X., A graphene-based broadband optical modulator. *Nature* **2011,** *474* (7349), 64-67; (b) Bao, Q.;

Loh, K. P., Graphene Photonics, Plasmonics, and Broadband Optoelectronic Devices. *ACS Nano* **2012,** *6* (5), 3677-3694; (c) Lemme, M. C.; Koppens, F. H. L.; Falk, A. L.; Rudner, M. S.; Park, H.; Levitov, L. S.; Marcus, C. M., Gate-Activated Photoresponse in a Graphene p–n Junction. *Nano Lett.* **2011,** *11* (10), 4134-4137.

5. (a) Yoon, H. J., et al., Sensitive capture of circulating tumour cells by functionalized graphene oxide nanosheets. *Nature Nanotech.* **2013,** *8* (10), 735-741; (b) Liu, J.; Cui, L.; Losic, D., Graphene and graphene oxide as new nanocarriers for drug delivery applications. *Acta Biomater.* **2013,** *9* (12), 9243-9257.

6. (a) Naebe, M.; Wang, J.; Amini, A.; Khayyam, H.; Hameed, N.; Li, L. H.; Chen, Y.; Fox, B., Mechanical Property and Structure of Covalent Functionalised Graphene/Epoxy Nanocomposites. *Sci. Rep.* **2014,** *4*; (b) Hwang, J.; Yoon, T.; Jin, S. H.; Lee, J.; Kim, T.-S.; Hong, S. H.; Jeon, S., Enhanced Mechanical Properties of Graphene/Copper Nanocomposites Using a Molecular-Level Mixing Process. *Adv. Mater.* **2013,** *25* (46), 6724-6729; (c) Goods, J. B.; Sydlik, S. A.; Walish, J. J.; Swager, T. M., Phosphate Functionalized Graphene with Tunable Mechanical Properties. *Adv. Mater.* **2014,** *26* (5), 718-723.

7. (a) Joshi, R. K.; Carbone, P.; Wang, F. C.; Kravets, V. G.; Su, Y.; Grigorieva, I. V.; Wu, H. A.; Geim, A. K.; Nair, R. R., Precise and Ultrafast Molecular Sieving Through Graphene Oxide Membranes. *Science* **2014,** *343* (6172), 752-754; (b) Wei, D., et al., Ultrathin rechargeable all-solid-state batteries based on monolayer graphene. *Journal of Materials Chemistry A* **2013,** *1* (9), 3177-3181; (c) El-Kady, M. F.; Kaner, R. B., Scalable fabrication of high-power graphene micro-supercapacitors for flexible and on-chip energy storage. *Nat. Commun.* **2013,** *4*, 1475.

8. (a) Choucair, M.; Thordarson, P.; Stride, J. A., Gram-scale production of graphene based on solvothermal synthesis and sonication. *Nature Nanotech.* **2009,** *4* (1), 30-33; (b) Paton, K. R.,

et al., Scalable production of large quantities of defect-free few-layer graphene by shear exfoliation in liquids. *Nature Mater.* **2014,** *13* (6), 624-630.

9. Edwards, R. S.; Coleman, K. S., Graphene synthesis: relationship to applications. *Nanoscale* **2013,** *5* (1), 38-51.

10. (a) Kim, K. S., et al., Large-scale pattern growth of graphene films for stretchable transparent electrodes. *Nature* **2009,** *457* (7230), 706-710; (b) Bae, S., et al., Roll-to-roll production of 30-inch graphene films for transparent electrodes. *Nature Nanotech.* **2010,** *5* (8), 574-578.

11. Yan, Z., et al., Rebar Graphene. *ACS Nano* **2014,** *8* (5), 5061-5068.

12. Coleman, J. N., Liquid Exfoliation of Defect-Free Graphene. *Acc. Chem. Res.* **2012,** *46* (1), 14-22.

13. (a) Economopoulos, S. P.; Tagmatarchis, N., Chemical Functionalization of Exfoliated Graphene. *Chem.–Eur. J.* **2013,** *19* (39), 12930-12936; (b) Kozhemyakina, N. V.; Englert, J. M.; Yang, G.; Spiecker, E.; Schmidt, C. D.; Hauke, F.; Hirsch, A., Non-Covalent Chemistry of Graphene: Electronic Communication with Dendronized Perylene Bisimides. *Adv. Mater.* **2010,** *22* (48), 5483-5487; (c) Basiuk, E. V.; Martinez-Herrera, M.; Alvarez-Zauco, E.; Henao-Holguin, L. V.; Puente-Lee, I.; Basiuk, V. A., Noncovalent functionalization of graphene with a Ni(ii) tetraaza[14]annulene complex. *Dalton Trans.* **2014,** *43* (20), 7413-7428; (d) Chua, C. K.; Pumera, M., Covalent chemistry on graphene. *Chem. Soc. Rev.* **2013,** *42* (8), 3222-3233.

14. Ramakrishna Matte, H. S. S.; Subrahmanyam, K. S.; Venkata Rao, K.; George, S. J.; Rao, C. N. R., Quenching of fluorescence of aromatic molecules by graphene due to electron transfer. *Chem. Phys. Lett.* **2011,** *506* (4–6), 260-264.

15. Kim, M.; Safron, N. S.; Huang, C.; Arnold, M. S.; Gopalan, P., Light-Driven Reversible Modulation of Doping in Graphene. *Nano Lett.* **2011,** *12* (1), 182-187.

16. K. C, C. B.; Das, S. K.; Ohkubo, K.; Fukuzumi, S.; D'Souza, F., Ultrafast charge separation in supramolecular tetrapyrrole-graphene hybrids. *Chem. Commun. (Cambridge, U. K.)* **2012,** *48* (97), 11859-11861.

17. Mann, J. A.; Rodríguez-López, J.; Abruña, H. D.; Dichtel, W. R., Multivalent Binding Motifs for the Noncovalent Functionalization of Graphene. *J. Am. Chem. Soc.* **2011,** *133* (44), 17614-17617.

18. Malig, J.; Jux, N.; Kiessling, D.; Cid, J.-J.; Vázquez, P.; Torres, T.; Guldi, D. M., Towards Tunable Graphene/Phthalocyanine–PPV Hybrid Systems. *Angew. Chem., Int. Ed.* **2011,** *50* (15), 3561-3565.

19. Mathew, S., et al., Dye-sensitized solar cells with 13% efficiency achieved through the molecular engineering of porphyrin sensitizers. *Nature Chem.* **2014,** *6* (3), 242-247.

20. D'Souza, F.; Ito, O., Supramolecular donor-acceptor hybrids of porphyrins/phthalocyanines with fullerenes/carbon nanotubes: electron transfer, sensing, switching, and catalytic applications. *Chem. Commun. (Cambridge, U. K.)* **2009,** *0* (33), 4913-4928.

21. Imahori, H.; Sekiguchi, Y.; Kashiwagi, Y.; Sato, T.; Araki, Y.; Ito, O.; Yamada, H.; Fukuzumi, S., Long-Lived Charge-Separated State Generated in a Ferrocene–meso,meso-Linked Porphyrin Trimer–Fullerene Pentad with a High Quantum Yield. *Chem.–Eur. J.* **2004,** *10* (13), 3184-3196.

22. Economopoulos, S. P.; Skondra, A.; Ladomenou, K.; Karousis, N.; Charalambidis, G.; Coutsolelos, A. G.; Tagmatarchis, N., New hybrid materials with porphyrin-ferrocene and

porphyrin-pyrene covalently linked to single-walled carbon nanotubes. *RSC Advances* **2013,** *3* (16), 5539-5546.

23. (a) Xu, Y.; Liu, Z.; Zhang, X.; Wang, Y.; Tian, J.; Huang, Y.; Ma, Y.; Zhang, X.; Chen, Y., A Graphene Hybrid Material Covalently Functionalized with Porphyrin: Synthesis and Optical Limiting Property. *Adv. Mater.* **2009,** *21* (12), 1275-1279; (b) Zhang, H.; Han, Y.; Guo, Y.; Dong, C., Porphyrin functionalized graphene nanosheets-based electrochemical aptasensor for label-free ATP detection. *J. Mater. Chem.* **2012,** *22* (45), 23900-23905; (c) Umeyama, T., et al., Preparation and Photophysical and Photoelectrochemical Properties of a Covalently Fixed Porphyrin–Chemically Converted Graphene Composite. *Chem.–Eur. J.* **2012,** *18* (14), 4250-4257.

24. Malig, J.; Romero-Nieto, C.; Jux, N.; Guldi, D. M., Integrating Water-Soluble Graphene into Porphyrin Nanohybrids. *Adv. Mater.* **2012,** *24* (6), 800-805.

25. (a) Georgakilas, V.; Otyepka, M.; Bourlinos, A. B.; Chandra, V.; Kim, N.; Kemp, K. C.; Hobza, P.; Zboril, R.; Kim, K. S., Functionalization of Graphene: Covalent and Non-Covalent Approaches, Derivatives and Applications. *Chem. Rev. (Washington, DC, U. S.)* **2012,** *112* (11), 6156-6214; (b) Pagona, G.; Sandanayaka, A. S. D.; Araki, Y.; Fan, J.; Tagmatarchis, N.; Yudasaka, M.; Iijima, S.; Ito, O., Electronic Interplay on Illuminated Aqueous Carbon Nanohorn−Porphyrin Ensembles. *J. Phys. Chem. B* **2006,** *110* (42), 20729-20732.

26. Zhang, X.-F.; Xi, Q., A graphene sheet as an efficient electron acceptor and conductor for photoinduced charge separation. *Carbon* **2011,** *49* (12), 3842-3850.

27. Cardona, C. M.; Li, W.; Kaifer, A. E.; Stockdale, D.; Bazan, G. C., Electrochemical Considerations for Determining Absolute Frontier Orbital Energy Levels of Conjugated Polymers for Solar Cell Applications. *Adv. Mater.* **2011,** *23* (20), 2367-2371.

28. Malig, J.; Stephenson, A. W. I.; Wagner, P.; Wallace, G. G.; Officer, D. L.; Guldi, D. M., Direct exfoliation of graphite with a porphyrin - creating functionalizable nanographene hybrids. *Chem. Commun. (Cambridge, U. K.)* **2012,** *48* (70), 8745-8747.

29. Economopoulos, S. P.; Rotas, G.; Miyata, Y.; Shinohara, H.; Tagmatarchis, N., Exfoliation and Chemical Modification Using Microwave Irradiation Affording Highly Functionalized Graphene. *ACS Nano* **2010,** *4* (12), 7499-7507.